

Sequential binding of large molecules to hairy MOFs†

Cite this: *Chem. Commun.*, 2013, **49**, 6641Gonghua Wang,^a Zhanping Xu,^a Ziguang Chen,^a Wei Niu,^b You Zhou,^c Jiantao Guo^b and Li Tan^{*a}Received 12th April 2013,
Accepted 24th May 2013

DOI: 10.1039/c3cc42711k

www.rsc.org/chemcomm

Metal–organic frameworks (MOFs) are entities with a repertoire of dynamic functions. With a simple touch of salts, smooth crystals of MOFs can be turned into hairy ones, dramatically enhancing chemisorption of large molecules, *i.e.*, by 120 times. When this process is followed by another round of etching, sequential binding of different proteins is possible.

Metal–organic frameworks (MOFs) are a class of sophisticated crystalline solids with well-defined coordination geometry and porosity.^{1–4} Rich selections of building blocks, long-range ordering in packing, and superior surface areas have promoted MOFs' applications in gas adsorption, storage, and separation.^{5–10} While most studies utilized inner pores by regulating their interactions with small molecules, MOFs are rarely reported to bind large molecules, for instance, polymers^{11–13} or proteins.^{14,15} Two major reasons are the limited pore sizes and chemical instability of the frameworks. Though expanded pores have been reported for hosting large molecules such as proteins,¹⁶ most of the MOFs have pore size spanning from several angstroms to a couple of nanometers.¹⁷ The size exclusion prevents large molecules from entering the inner pores, and hence they stick to the outer surfaces only.¹⁸ Chemical instability makes MOFs vulnerable when in contact with liquid media such as water and organic solvent, through ligand exchange processes.^{19–23} A combination of both factors therefore makes a controlled binding of large molecules challenging.

We recently found that defects like cracks or edges in MOFs are effective traps for retaining large molecules like proteins (Fig. 1A). A simple mechanical crushing reveals more active sites and greatly enhances protein adsorption onto particular crystal planes (Fig. 1B–E; ESI†). To push this discovery further,

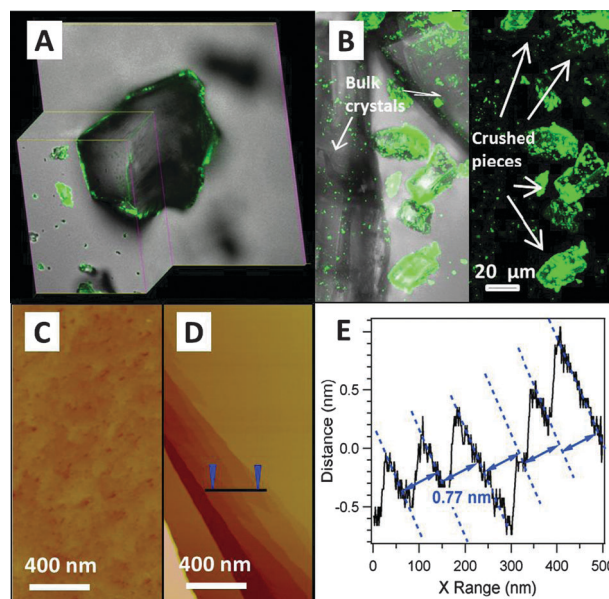


Fig. 1 Confocal fluorescent microscopic images of protein (GFPs) adhesion on (A) bulk and (B) crushed Cu-MOF crystals; AFM images of (C) the bulk and (D) crushed MOF crystal; (E) section analysis of (D) along the line revealing the surface terraces with a fringe spacing of 0.77 nm, matching crystal planes of (200) (see ESI† for detailed analysis).

we report sequential binding of large molecules on this same type of MOFs *via* salt etching, as illustrated in the Table-of-Contents graphic.

Our MOFs, dubbed as Cu-MOFs, are assembled in an interpenetrating pseudo-cubic crystal structure, with pure Cu–O bonded (200) layers and pillar-like units between the layers¹⁰ (Fig. S1 and Table S1, ESI†). The etching process was performed to break the (200) layers and we investigated the effects using an atomic force microscope (AFM). Prior to imaging, these MOFs were treated with a series of salt solutions, *e.g.*, 0.57, 5.7, 57 and 570 mM, respectively, for 10 minutes. The height images of the four crystal surfaces (Fig. 2) revealed an enhanced surface roughening as the salt concentration increased. When the crystals were treated with the most diluted salt solution

^a Department of Mechanical and Materials Engineering, University of Nebraska, Lincoln, Nebraska 68588, USA. E-mail: ltan4@unl.edu; Tel: +1 4024724018

^b Department of Chemistry, University of Nebraska, Lincoln, Nebraska 68588, USA

^c Center for Biotechnology, University of Nebraska, Lincoln, Nebraska 68588, USA

† Electronic supplementary information (ESI) available: Details of materials synthesis and characterization, AFM data analysis, XRD patterns of the copper compounds, SEM and confocal fluorescent microscopic images. See DOI: 10.1039/c3cc42711k

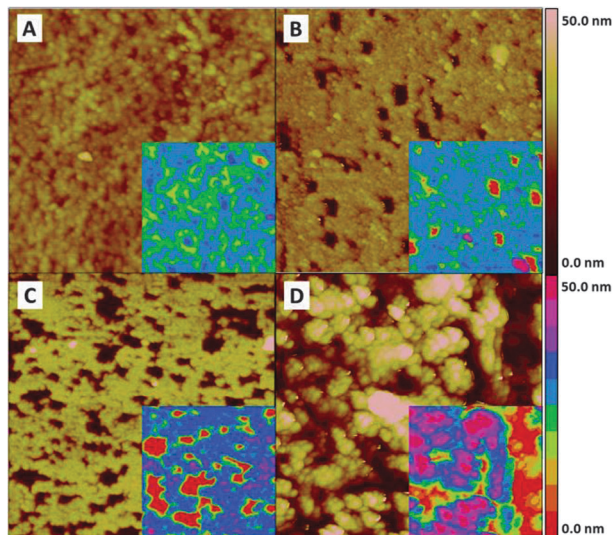


Fig. 2 AFM images of Cu-MOFs treated with NaCl solutions with concentrations of (A) 0.57, (B) 5.7, (C) 57 and (D) 570 mM. All images are $2\ \mu\text{m} \times 2\ \mu\text{m}$ in size. The continuous and the sectional color scales are shown on the right side.

(0.57 mM), their smooth surfaces became densely bumpy ones, with the surface roughness increased from 0.82 to 3.02 nm (Fig. 1C and 2A, Table S2, ESI[†]). When the salt concentration increased by 10 times, discrete rectangular-shaped pit holes emerged (Fig. 2B). As the salt concentration further increased by 100 times, many more pit holes appeared and some of them grew into larger ones, indicating possible migration of crystal grains (Fig. 2C). When the crystals were soaked in a 570 mM salt solution, trenches appeared, further indicating possible surface or subsurface reconstructions (Fig. 2D). The statistical analysis of the peak to peak distances and void space volumes, based on the height histograms, also suggests that our etching process expedites with increasing salt concentration (Fig. S2 and Table S2, ESI[†]).

Hairy MOFs show up when we impregnate the Cu-MOF crystals in a salt solution (57 mM) for an extended period of time, *e.g.*, from 30 min to 24 h. We found that the morphology of the crystals continuously evolves as the etching proceeds (Fig. 3). After a 30 min soaking, a large number of pit holes appear, consistent with our earlier AFM observations in Fig. 2C. Right after 24 h, these crystals were covered with populated clusters of rods, with cross-section dimensions in the range of 200–300 nm and lengths of approximately $15\ \mu\text{m}$ (Fig. 3A). A careful view of the hair roots reveals a grain size of 50 nm (Fig. 3B), suggesting reorganization of 4–5 of these into one larger rectangular hair. Often, this volume change in internal structure can twist the fibres into helical structures (Fig. 3C). Overall, the shiny green crystals turned opaque and furry under the lens of an optical microscope (Fig. 3D). When the rod clusters, dubbed as hairy MOFs or H-MOFs, are placed in a GFP solution, substantial fluorescence is detected, suggesting a strong affinity of H-MOFs for protein molecules (Fig. 3E). In contrast to pristine Cu-MOFs, given the rod size in Fig. 3B and a density of $10\ \text{rods}\ \mu\text{m}^{-2}$, salt-etching yields 120 times more contact area for molecule-binding.

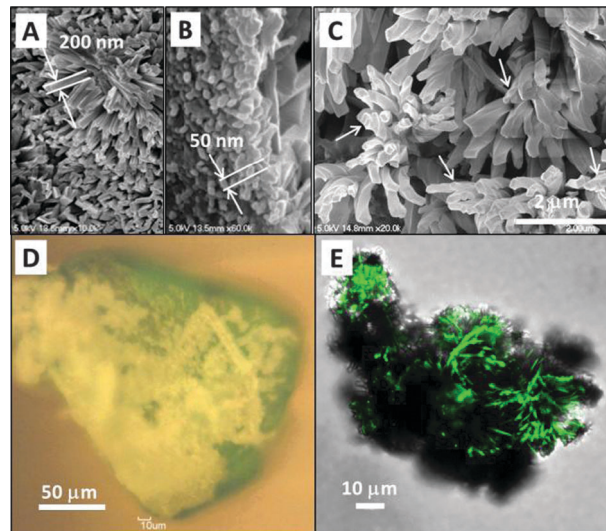


Fig. 3 The morphological evolution of H-MOFs and enhanced surface GFP adhesion. SEM images of Cu-MOFs after soaking in a NaCl solution (57 mM) for (A) 30 min, (B) 24 h. (C) Roots of the fibers in (B) reveal 50 nm sized grains. (D) Optical microscopic image of the H-MOFs in (B). (E) Confocal fluorescent microscopic images of GFP-coated hairy MOFs.

While the interaction between hairy MOFs and GFPs provides hints of copper–protein binding, a challenge remains in identifying the structure of H-MOFs. We first probed the porous feature of H-MOFs by examining their gas sorption properties. The N_2 sorption isotherms, compared to the ones for Cu-MOFs,¹⁰ show negligible N_2 sorption, indicating the breaking of the interpenetrating microporous framework of Cu-MOFs after salt etching (Fig. S3, ESI[†]). The CO_2 sorption isotherm of H-MOFs (Fig. S3D, ESI[†]), showing the sorption capacity about half of that absorbed by Cu-MOFs (Fig. S3B, ESI[†]), also suggests the cleaved framework structure of H-MOFs.

We further synthesized a series of crystalline materials containing different combinations of Cu, fumarate (FMA^{2-}) and 4,4'-Bpe (see details in ESI[†]). Comparison of XRD patterns (Fig. S4, ESI[†]) shows that H-MOFs have a similar crystal structure to $\text{CuCl}_2(4,4'\text{-Bpe})$, and elemental analysis yields a composition of C: 45.59%, H: 3.12%, N: 8.82%, and Cl: 22.54%. It is worth noting that there are a few extra XRD peaks at 16.5° , 19.4° , 20.3° and 25.7° , suggesting the existence of CuFMA .²⁴ Therefore, the hairy MOFs contain ingredients of both $\text{CuCl}_2(4,4'\text{-Bpe})$ (major) and CuFMA (minor). We hypothesize that the salt etching has modified the (200) planes in Cu-MOFs. Immediately after NaCl is introduced into the mother liquid of Cu-MOFs, the burst of Na^+ ions can disrupt the dynamic equilibrium of the MOF crystals and their mother liquid by depriving them of the fumarate moieties which are chelated to the copper centers in the (200) planes. As a consequence, the leaching of fumarate, which is the main building block of (200) planes, unavoidably triggers the transformation of layered structures into fine fibers. Meanwhile, the Cu–N bonds adapt to these changes and reorganize the newly introduced species, namely chloride ions, to form the emerald-coloured $\text{CuCl}_2(4,4'\text{-Bpe})$. Since the entire etching process is performed at room temperature, some CuFMA can precipitate out as a side-product.

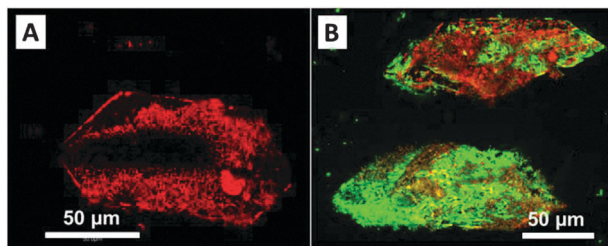


Fig. 4 Confocal fluorescent microscopic images of H-MOFs (A) after soaking in RFP solution for 1 week and (B) after a second soaking in NaCl solution and followed by soaking in GFPs solution.

Moreover, we evaluated the increased active copper sites by comparing fluorescent response from $\text{CuCl}_2(4,4'\text{-Bpe})$ and CuFMA respectively. Although both materials exhibit rod-like structures (Fig. S5A and S5D, ESI[†]), the confocal microscopic image of $\text{CuCl}_2(4,4'\text{-Bpe})$ in GFP solution reveals bright fluorescent signals all through the solids (Fig. S5B and S5C, ESI[†]), while the CuFMA rods show hardly any fluorescent response (Fig. S5E and S5F, ESI[†]). This comparison clearly indicates that $\text{CuCl}_2(4,4'\text{-Bpe})$ in H-MOFs is indeed the compound that is active in binding GFPs, not CuFMA. We further extended the salt etching protocol with common biological media. In parallel, we compared the behaviors of Cu-MOF and hairy MOFs in Dulbecco's Modified Eagle Medium (DMEM) with added fetal bovine serum (FBS) and GFPs. Unsurprisingly, site-selective fluorescent signals are found in this alternative experiment, while strong affinity of FBS on copper-rich hairy MOFs confirms intense and uniform adhesion of GFPs (Fig. S6, ESI[†]).

Now, we apply this etching process to bind large molecules in a stepwise manner (for a schematic representation see the Table-of-Contents figure). Particularly, we used RFPs and GFPs alternately after every individual etching process. After one day of reaction with NaCl solution, rod-like features grew on hairy MOFs and they showed a strong interaction with RFPs, as in Fig. 4A. After the removal of unbound RFPs and another round of salt etching, a new protein, *i.e.*, GFP, was used to decorate the solids. Correspondingly, the confocal fluorescent microscopic image shows added but distinguishable green fluorescent signals (Fig. 4B). Comparison of these signals with those of the fresh $\text{CuCl}_2(4,4'\text{-Bpe})$ rods, which contain rather fixed surface copper sites, shows that the H-MOFs are able to expose new sites after binding. In addition, the site-selective sequential binding results present a different binding motif from the hydrophobic-hydrophobic interaction reported in the MOFs with large pore sizes.¹⁶

In summary, we have chemically engineered Cu-MOFs towards enriched Cu binding sites with a touch of salt. Analogous to the expedited rusting of iron in seawater, saltwater can also accelerate the "corrosion" of crystalline Cu-MOFs. The salt solutions promoted the solvation and extraction of fumaric species from the original framework and delivered highly dense

rod-like structures. Engineered hairy MOFs have demonstrated 120 times more enhanced binding of GFPs, as well as the capability of stepwise binding. Through this consecutive and selective binding, H-MOFs can serve as a microreactor for various biomolecular reactions. In addition, as metal-protein binding is a major contributor to the rigidity of electron transfer in many biochemical processes, we envision that our work is beneficial to broad areas of biological research.¹⁹

The authors gratefully acknowledge the financial support from the National Science Foundation, Nebraska Research Initiative, and Nebraska Center for Energy Science Research. We also thank Jingzhi Lu and Dr Jian Zhang for gas sorption measurements and helpful discussion.

Notes and references

- 1 N. Stock and S. Biswas, *Chem. Rev.*, 2012, **112**, 933–969.
- 2 H. C. Zhou, J. R. Long and O. M. Yaghi, *Chem. Rev.*, 2012, **112**, 673–674.
- 3 O. M. Yaghi, M. O'Keeffe, N. W. Ockwig, H. K. Chae, M. Eddaoudi and J. Kim, *Nature*, 2003, **423**, 705–714.
- 4 D. Zacher, R. Schmid, C. Woll and R. A. Fischer, *Angew. Chem., Int. Ed.*, 2011, **50**, 176–199.
- 5 R. E. Morris and P. S. Wheatley, *Angew. Chem., Int. Ed.*, 2008, **47**, 4966–4981.
- 6 J. R. Li, J. Sculley and H. C. Zhou, *Chem. Rev.*, 2012, **112**, 869–932.
- 7 M. P. Suh, H. J. Park, T. K. Prasad and D. W. Lim, *Chem. Rev.*, 2012, **112**, 782–835.
- 8 N. L. Rosi, J. Eckert, M. Eddaoudi, D. T. Vodak, J. Kim, M. O'Keeffe and O. M. Yaghi, *Science*, 2003, **300**, 1127–1129.
- 9 P. Horcajada, R. Gref, T. Baati, P. K. Allan, G. Maurin, P. Couvreur, G. Ferey, R. E. Morris and C. Serre, *Chem. Rev.*, 2012, **112**, 1232–1268.
- 10 B. L. Chen, S. Q. Ma, F. Zapata, F. R. Fronczek, E. B. Lobkovsky and H. C. Zhou, *Inorg. Chem.*, 2007, **46**, 1233–1236.
- 11 X. Q. Liang, F. Zhang, W. Feng, X. Q. Zou, C. J. Zhao, H. Na, C. Liu, F. X. Sun and G. S. Zhu, *Chem. Sci.*, 2013, **4**, 983–992.
- 12 M. D. Rowe, D. H. Thamm, S. L. Kraft and S. G. Boyes, *Biomacromolecules*, 2009, **10**, 983–993.
- 13 T. Ben, C. J. Lu, C. Y. Pei, S. X. Xu and S. L. Qiu, *Chem.–Eur. J.*, 2012, **18**, 10250–10253.
- 14 R. Y. Tsien, *Annu. Rev. Biochem.*, 1998, **67**, 509–544.
- 15 H. Morise, O. Shimomura, F. H. Johnson and J. Winant, *Biochemistry*, 1974, **13**, 2656–2662.
- 16 H. X. Deng, S. Grunder, K. E. Cordova, C. Valente, H. Furukawa, M. Hmadeh, F. Gandara, A. C. Whalley, Z. Liu, S. Asahina, H. Kazumori, M. O'Keeffe, O. Terasaki, J. F. Stoddart and O. M. Yaghi, *Science*, 2012, **336**, 1018–1023.
- 17 J. X. Liu, B. Lukose, O. Shekhan, H. K. Arslan, P. Weidler, H. Gliemann, S. Brase, S. Grosjean, A. Godt, X. L. Feng, K. Mullen, I. B. Magdau, T. Heine and C. Woll, *Sci. Rep.*, 2012, **2**, 921.
- 18 M. Kondo, S. Furukawa, K. Hirai and S. Kitagawa, *Angew. Chem., Int. Ed.*, 2010, **49**, 5327–5330.
- 19 D. Maspoth, D. Ruiz-Molina, K. Wurst, N. Domingo, M. Cavallini, F. Biscarini, J. Tejada, C. Rovira and J. Veciana, *Nat. Mater.*, 2003, **2**, 190–195.
- 20 C. Mellot-Draznieks, C. Serre, S. Surble, N. Audebrand and G. Ferey, *J. Am. Chem. Soc.*, 2005, **127**, 16273–16278.
- 21 C. Serre, C. Mellot-Draznieks, S. Surble, N. Audebrand, Y. Filinchuk and G. Ferey, *Science*, 2007, **315**, 1828–1831.
- 22 M. Kim, J. F. Cahill, H. Fei, K. A. Prather and S. M. Cohen, *J. Am. Chem. Soc.*, 2012, **134**, 18082–18088.
- 23 J. An and N. L. Rosi, *J. Am. Chem. Soc.*, 2010, **132**, 5578–5579.
- 24 M. E. Zaballa, L. A. Abriata, A. Donaire and A. J. Vila, *Proc. Natl. Acad. Sci. U. S. A.*, 2012, **109**, 9254–9259.